Investigation of Travel Interference Problems in Taxi-Type AGV Transport Systems and Its Estimation under SLAM Operations

Tomoya A. Matsui *, Yasuaki B. Omi, Toshiki C. Hirogaki, and Eiichi D. Aoyama

Graduate School of Science and Engineering, Department of Mechanical Engineering, Doshisha University, Kyoto, Japan

Email: ibl53985398@gmail.com (T.A.M.); yasuaki4191@icloud.com (Y.B.O.); thirogak@mail.doshisha.ac.jp (T.C.H.); eaoyama@mail.doshisha.ac.jp (E.D.A.)

*Corresponding author

***Abstract*—Automated Guided Vehicles (AGVs) are becoming increasingly important in flexible manufacturing systems because they can adapt to changes in facilities and factory layouts. However, AGV transport systems suffer from system shutdowns when the AGVs collide. In this study, our objective was to investigate how the interference time of taxi-type AGV transport systems is altered when a passing place is installed at the pick-up and drop-off points (P/Ds) to reduce the interference between AGVs. Consequently, it was inferred that the main cause of interference during taxi-type autonomous driving was when the AGV, a type of autonomous mobile robot, waited at the P/D, and installing the passing place was effective. In recent years, there has also been a growing trend toward autonomous AGVs that use simultaneous localization and mapping for self-position estimation and environmental mapping. In autonomous driving, a high level of self-position estimation is important because it is related to interference between AGVs. However, the accuracy of AGV self-position estimation depends on the environment in which the AGV is used and its traveling speed. Therefore, our objective was to evaluate the accuracy of self-position estimation when the environment was used and the AGV speed was varied. The results demonstrated that the speed and standard deviation were positively correlated. The standard deviation was smaller for the rectangle (b) than the wall (a) on both sides. Therefore, the possibility of interference between AGVs increases when the speed is high or when there are few features, such as walls, because the accuracy of self-position estimation decreases.**

***Keywords*—Automated Guided Vehicles (AGVs), taxi, transportation system, travel interference, Simultaneous Localization and Mapping (SLAM), self-position estimation**

I. Introduction

As market needs change, production systems shift from low-mix, high-volume production to high-mix, low-volume production, as typified by Flexible Manufacturing Systems (FMS). However, in an FMS, the entire production system is hierarchically controlled as a large-scale problem; therefore, once the system is built, it is difficult to change the equipment or layout in the factory. Variable-mix and variable-volume production systems have been proposed to solve these problems. For example, autonomous decentralized production systems exist in which the components of the production system have autonomous decision-making functions [1, 2]. Among the components of these systems, Automated Guided Vehicle (AGV) transport systems, which control the flow of goods in factories, are expected to become increasingly important. The design of the system and its operation strategy can produce considerable differences in production efficiency. Although AGVs can respond flexibly to various transport conditions, their production efficiency can be reduced because of interference problems between AGVs when multiple AGVs are operated. Previous studies have been conducted to avoid interference between AGVs because this serious problem can cause system shutdowns [3, 4]. Therefore, it is important to develop system design algorithms and operational strategies that ensure efficient and stable transportation. Strategic control methods consider the flexibility and optimality of AGV transport systems [5], AGV behavioral decision theory with future predictive reasoning problems [6], simultaneous scheduling methods for processing machines and multiple-load AGVs using genetic algorithms [7, 8], and cellular automaton methods that can reproduce the phenomena of complex systems based on the local neighborhood rule [9, 10]. Research is actively being conducted to develop autonomous systems. Research is also being conducted on the autonomous movement of AGVs, such as transport systems, in which AGVs autonomously generate a route and move to a destination without guidance [11] or autonomous travel guidance to avoid obstacles in dynamic environments [12]. However, a more efficient system design is still required, and practical algorithms for an efficient system design and operational strategies for stable operation are yet to be fully established. Therefore, developing algorithms for the AGV system

Manuscript received July 10, 2023; revised August 1, 2023; accepted October 25, 2023; published April 26, 2024.

design and research strategies for system operation is essential.

In recent years, cross-industrial research has been actively conducted to create novel knowledge in the industrial world. Novel attempts in academic research have been made to mimic the superior functions of living organisms (biomimetics); these attempts have been applied to material industries [13, 14]. However, these studies have focused on transportation engineering, a research field different from production engineering, especially regarding the mobility characteristics of taxis, which have high flexibility and are the subject of much research, such as novel operation systems. By mimicking these behavioral characteristics, researchers are studying AGV transport systems that are more efficient and can flexibly respond to changes in location. In recent years, AGVs have been introduced in locations other than production plants, such as Amazon's distribution center and Amazon Kawasaki FC [15]. On these distribution sites, AGVs automatically unload products that are ordered online. The number of shelves in a logistics center varies depending on the industry, but one online shopping company can manage approximately 5,000–10,000 different products with 7,000–30,000 storage shelves [16]. The number of customer order slips per day could reach approximately 30,000. Therefore, there is a strong need for an AGV transport system that can create shipping plans on time to meet delivery deadlines for customer orders and cope with environments in which the point of origin and destination of transported goods differ from case to case. Under such circumstances, it would be effective to apply the running characteristics of taxis to AGVs that constantly change the points at which passengers are picked and dropped.

The basic rules of conduct for taxi-type AGVs, which are Autonomous Mobile Robots (AMR), include waiting and cruising. During the waiting operation, the AGV stands at the waiting pick-up and drop-off stations (P/Ds) and runs when a load is generated. Taxes in the field empirically use these two methods to acquire passengers efficiently. However, only a few studies have been conducted on the combined use of taxi-type AGVs in waiting and cruising operations. This study introduces a grouping method called clustering for combining waiting and cruising operations.

In AGV transport systems, the system stops when the AGVs collide, which is a problem. In this study, to reduce the interference time between AGVs, a passing point was established at the waiting business location. This study attempts to investigate the effect of providing an egress point at the waiting business location of AGVs on the reduction in interference time in taxi-type AGV control.

Also, in recent years, there has been a growing trend toward autonomous AGVs that use Simultaneous Localization and Mapping (SLAM) for self-position estimation and environmental mapping [17]. In autonomous driving, a high level of self-position estimation is important because it is related to interference between AGVs. However, the accuracy of AGV self-position estimation depends on the environment in which the AGV is used and its traveling speed. Therefore, this experiment attempts to investigate the accuracy of self-position estimation when the environment and speed at which the AGVs are used vary.

The remainder of this paper is organized as follows. Section II describes taxi travel characteristics, and Section III describes the clustering and internode travel time. Section IV describes the SLAM operations. The experimental procedures for taxi-type AGV and SLAM operations are presented in Sections V and VI, respectively. Finally, the results and discussion, and summary are presented in Sections VII and VIII, respectively.

II. Taxi Travel Characteristics

A. Similarities between Transportation and Transport Systems

To apply knowledge from transportation systems to transport systems, it must be assumed that the transportation system has excellent mobility characteristics and that the surrounding environments are similar. Table I compares the evolution of the production and transportation systems. Transportation systems have a longer history than production systems and are believed to have evolved to an optimum state by overcoming various problems. Furthermore, as market needs have diversified, more flexible systems have emerged to meet these needs, and environmental conditions are considered similar. Fig. 1 illustrates the characteristics of typical transportation and transport equipment systems, focusing on their flexibility.

TABLE I. Transition of Traffic System and Manufacturing Systems

	18th century	19th century	20th century	
Traffic system	Watt steam engine appearance	1872 The railway opens a business	1903 The bus opens a business	1912 The taxi opens a business
Manufacturing system			1946 Manufacturing method of a large amount of small types	1970 Manufacturing method of a small amount of several varieties

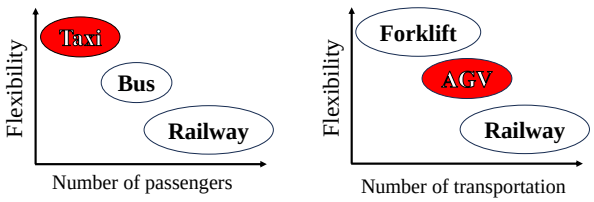

(a) Traffic system (b) Conveyance system

Fig. 1. Comparison of flexibility and number of passengers.

As illustrated in Fig. 1(a), taxis as transportation equipment in transportation systems are characterized by their high flexibility. However, the amount of transportation per trip is less than that of buses and railroads. As illustrated in Fig. 1(b), conveyors, AGVs, and forklifts are the most flexible transport devices for

production systems. Because an autonomous transport system requires a flexible and efficient unmanned system, applying the highly flexible mobility characteristics of taxis to the behavioral laws of AGVs is considered effective.

B. Job, AGV, and Guide Path Conditions

The job generation and transportation settings in this study are detailed in (1) and (2), respectively.

(1) The points at which jobs are generated at each P/D are randomly determined. The pick-up and drop-off stations (P/Ds) are the points at which the AGV receives a job.

(2) The destination of the job is assumed random and unknown until the AGV receives it.

The behavioral rules and constrains of the AGV and the travel-lane conditions are detailed subsequently.

(1) The travel lane is a single-lane single-directional guide path.

(2) When a job occurs, the nearest AGV that did not receive a command obtains it.

(3) AGV travels the shortest route to its destination.

(4) AGVs are not allowed to travel in the reverse direction of the travel lane.

(5) One AGV cannot overtake another.

(6) AGVs do not know the positions or situations of other AGVs. Therefore, a detour cannot be taken to avoid deadlocks.

(7) The number of jobs an AGV can perform is limited to one.

The states of the AGVs are illustrated in (a)–(c) below.

(a) S1: The AGV receives a command and selects the job that has been generated.

(b) S2: AGV transport jobs.

(c) S3: AGV finishes transporting the job and waits for a command.

Fig. 2 presents the AGV algorithm used here.

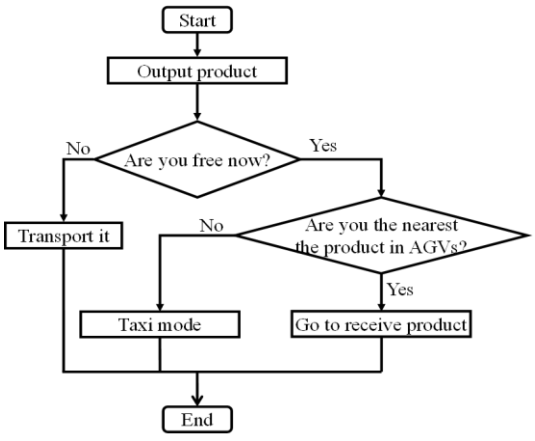

Fig. 2. Algorithm of AGV system based on taxi characteristics.

III. Clustering and Inter-Node Travel Time

A. Application of Clustering to Taxi-Type AGVs

Clustering is a data-analysis method that divides a set into subsets based on certain evaluation criteria. In this experiment, we used a hierarchical method, which is used when the amount of data is small, to classify P/Ds that are close to each other in terms of distance, thus combining the waiting and cruising operations. Hierarchical clustering groups the P/Ds in order of proximity, resulting in a tree diagram, as illustrated in Fig. 3.

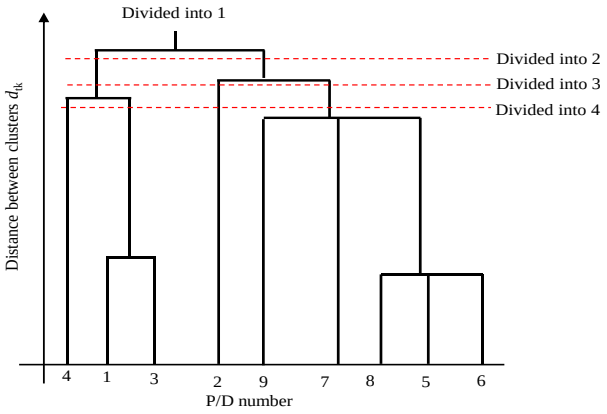

Fig. 3. Tree diagram in hierarchical clustering.

B. How to Dispatch Vehicles for Waiting and Cruising Operations

The tree diagram obtained from the clustering was used to allocate vehicles for waiting and cruising operations. In the tree diagram presented in Fig. 3, the clusters can be divided stepwise by cutting the tree from the top of the tree diagram. The number of AGVs assigned to a cluster was the number of AGVs divided by the number of clusters. If the number of AGVs is indivisible by the number of clusters, more AGVs are allocated to clusters with larger patrol route lengths, and only one AGV can be allocated to the waiting operation P/D. Table II presents an example of an AGV dispatching up to Cluster 4.

TABLE II. AGV Allocation

	Divided into 2		**Divided into 3**			**Divided into 4**			
Patrol route P/D	①③④	②⑨⑤⑦⑧⑥	①③④	②	⑤⑧⑨⑦⑥	①③	②	④	⑤⑧⑨⑦⑥
Number of AGVs	2	2	1	1	2	1	1	1	1

C. AGV Behavior Rule after Clustering

The cruising operation behavior when clustering is introduced are detailed subsequently.

(1) AGVs classify P/Ds close to each other by clustering and continue to patrol the classified P/Ds in the shortest possible time. Dijkstra's method was used to determine the patrol routes.

(2) When a transported object is generated, the AGV in the non-transporting state closest to the object's location moves to pick up the object, regardless of the assigned patrol route.

(3) The load's destination was not affected by clustering, and the load was transported to a random P/D.

(4) If an AGV transports an object outside its assigned circuit, it returns to its original circuit after the transport. In other words, the AGVs do not move between the assigned flow circuits.

Similarly, the clustering-based waiting operation behavior rules are detailed subsequently.

(1) Clustering is used to classify P/Ds close to each other, and the AGV waits for the classified P/D to become a waiting sales P/D.

(2) When a transported object is generated, the AGV in the non-transporting state closest to the location where the object is generated selects the object.

(3) The destination of the transported object is unaffected by clustering, and the object is transported to a random P/D.

(4) After transportation, the AGV waits for the original waiting P/D.

D. Clustering Method

A previous study determined that the group average method can divide the P/D while capturing course characteristics and efficiently incorporating taxi travel characteristics into AGVs [18]. Therefore, the group-average method was used as the clustering method in this study.

In the group averaging method, the average distance between samples of all combinations of clusters is used as the distance between clusters. Fig. 4 illustrates the group-averaging method. This definition is given in Eq. (1).

$$d_{TK} = \frac{1}{n_T n_K} \sum_{p \in C_T, q \in C_k} d_{pq} \quad (1)$$

where n_T and n_K are the numbers of objects in clusters C_T, C_K, and d_{pq} is the distance between the clusters of objects in clusters C_T and C_K.

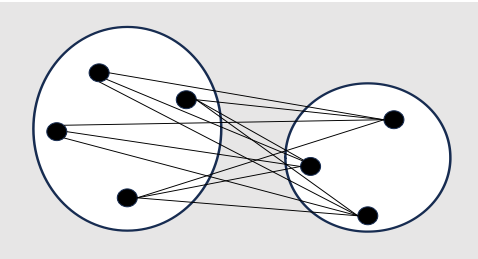

Fig. 4. Group average method and tree diagram.

E. Clustering Node-to-Node Travel Time

Because the AGV travel time depends on the scale of the course layout and AGV speed v, the AGV travel time is expressed as a dimensionless quantity. The representative length is the distance between nodes L_n, the smallest unit of the AGV path selection, and the representative speed is the AGV speed v. The travel time between nodes T_n is expressed as Eq. (2).

$$T_n = \frac{L_n}{v} \quad (2)$$

IV. SLAM Operations

A. SLAM

SLAM refers to the simultaneous estimation of self-positioning and environmental mapping by processing the data collected from sensors mounted on a robot [19]. SLAM technology is used in various applications such as AGVs, robots, and automatic driving. In this study, LiDAR SLAM with laser range scanners (LiDARs) was used.

B. Particle Filters

One ROS meta-package is the Navigation Stack, which provides the Adaptive Monte Carlo Localization (AMCL) with an ROS node. The AMCL algorithm is based on the Monte Carlo Localization (MCL) [20] using a particle filter. Fig. 5 presents the particle filter algorithm. The particle filter comprises three steps: (1) predicting the prior probability at time t based on the motion prediction from the motion model for particles at time t-1; (2) calculating the likelihood of each particle based on the data observed by sensors, etc., and assigning weights; (3) Resampling each particle based on its weight [21].

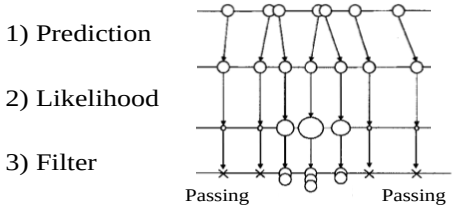

Fig. 5. Particle filter algorithm.

V. Experimental Procedure of Taxi-Type AGV

A. Purpose of Experiment

When an AGV runs on only one taxi route, it is biased toward a certain route, causing an oversupply or shortage of P/Ds in some areas. According to the "Survey on Safety Management in Taxi Business" conducted by the Ministry of Land, Infrastructure, Transport, and Tourism, actual cruising operation taxis are also over- or under-supplied locally because taxi drivers are biased toward routes with high occupancy rates. Recently, research has been conducted on optimal taxi dispatch control using clustering. In a previous study, clustering was applied to AGVs to solve the multiple traveling salesman problem, in which multiple AGVs shared all P/Ds. This study investigates how providing the passing place at the waiting business location of AGVs reduces interference time in taxi-type AGV control.

B. Experimental Device

The simulation software used here was the DELMIA/QUEST (ver. D5R19), manufactured by Dassault. The data obtained from this production simulator included the simulation time, average utilization rate of the elements (components of the logistics path, such as AGVs, job origination points, and transport destinations), average job dwell time, maximum waiting time, minimum waiting time, and total number of jobs that passed or were

transported. The production simulator displays the operational status and results in real time, allowing the user to visually grasp the transfer process of each AGV and identify problems in realizing a highly efficient transfer. In addition, the relationship between the shape and distance can be changed to a time relationship, depending on the speed of the AGV.

C. Flow Path Model Setup

Because conventional-type layouts are widely used in production, a grid layout with four vertical and four horizontal single-directional guide paths was adopted for the warehouses. Because goods are grouped by location in a distribution warehouse, we consider that a P/D is necessary for each grid. Therefore, we arranged the P/Ds such that at least one P/D was on each side of the grid. The flow path model used in the experiment and the arc node diagram of the course are presented in Fig. 6. The flow path size was set to 225×225 m, and the distance between the nodes, Ln, the minimum unit for the AGV runway selection, was set to 75 m. The course size was based on a large-scale warehouse. The course size was set to be 20000 m^2 or larger, which is the standard for large-scale warehouses. The travel speed of the AGVs was set to 1 m/s, which is the current limit for the maximum travel speed of AGVs in Japan. As the AGV runs on a unidirectional guideway, the outbound and inbound routes between the P/Ds and travel times differ. The flow path is represented by a path and decision point, and a pick-up and drop-off station (P/D) is located in the area enclosed by the guide path. Table III presents the relationship between the distance P/D and the average speed of the AGV and T_n. The Manhattan distance, L_{st}, was obtained using Eq. (3).

$$L_{st} = \sum_{q=0}^{n} \left(\left| x_{pq} - x_{p(q+1)} \right| + \left| y_{pq} - y_{p(q+1)} \right| \right) \tag{3}$$

$$\left(x_{p0}, y_{P0} \right) = \left(x_s, y_s \right)$$

The AGV travels the Manhattan distance between the P/Ds, where s is the starting P/D number; t is the destination P/D number; x_p and y_p are the junctions between the starting and destination P/Ds; and q is the passing order number of the junctions. The AGV travels the Manhattan distance between P/Ds. The AGV delivers and receives goods at P/D Stations 1–9, and the number of goods transported by the AGV at a given time is assumed to be one. The destination P/D was selected randomly to evaluate the transport performance under more uncertain conditions.

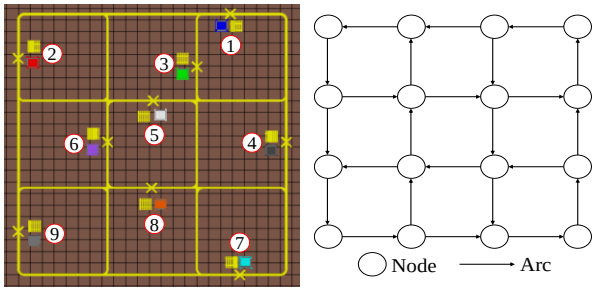

Fig. 6. Flow path model and ark node diagram.

TABLE III. TRANSPORT TIME MATRIX BETWEEN P/D

From P/D No. [-] \ To P/D No. [-]	1	2	3	4	5	6	7	8	9
1		2.859	0.953	5.815	4.769	3.813	3.797	2.825	4.789
2	5.027		5.980	6.899	1.969	4.899	4.881	3.909	1.989
3	2.932	5.791		4.861	3.816	2.860	2.843	1.871	3.836
4	2.072	4.929	3.025		6.841	5.885	5.868	4.896	6.860
5	3.059	5.859	4.012	4.929		2.929	2.913	1.940	3.905
6	4.015	2.929	4.968	5.900	0.956		3.868	2.896	4.861
7	4.088	6.889	5.041	2.017	4.916	3.960		2.971	4.935
8	5.108	3.920	5.956	6.875	1.945	0.989	4.857		1.965
9	6.983	5.897	7.935	4.968	3.923	2.967	2.951	5.864	

D. Passing Place

Fig. 7 presents the passing locations used in this study [22]. These are provided for P/Ds conducting waiting operations. Experiments were conducted with and without passing places, and the interference time rates were compared.

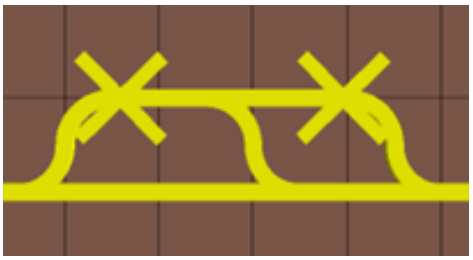

Fig. 7. Passing place model.

E. Experimental Conditions

Clustering was applied to the course illustrated in Fig. 6, from one to four divisions, to introduce the taxi travel characteristics. The clustering method used was the group average method, which exhibited the highest efficiency value in previous studies. In this section, a novel normal-mode AGV is used to examine the effect of clustering on the transport performance. Normal operation implies that an AGV that has completed transporting a job waits on the spot until a request to transport the next job is received.

Next, the evaluation function is discussed. The interference time is defined as when an AGV is close to another AGV and cannot move further. Interference includes interference between AGVs passing through intersections and interference between AGVs waiting at P/Ds. Because the magnitude of the interference depends on the experimental conditions, such as the interval between the occurrence of the objects to be transported, the ratio of the interference time to the AGV travel time was used as the evaluation function. This is the interference time rate, as expressed in Eq. (4).

$$R_b = \frac{T_\mathrm{b}}{T_\mathrm{r}} \tag{4}$$

In Eq. (4), T_b is the interference time between the AGVs and T_r is the running time of the AGVs.

The experimental conditions are listed in Table IV. The system was operated for 30,000 s (approximately 8 h, assuming one of three daily shifts). A warm-up period of 2,000 s (assumed to begin approximately 30 min after each

shift) was provided to obtain the output values of the system during steady operation, which were measured thereafter. The system-wide transport occurrence interval T_I was varied every 50 s from 200 to 500. However, for this discussion, the product interval was considered non-dimensionalized by dividing it by T_n. Comparative experiments were conducted between Clusters 2 and 4, in which clustering was applied to the course and normal modes. The effect of passing location on the interference time rate was also tested.

TABLE IV. EXPERIMENTAL CONDITIONS OF SIMULATION OF TAXI-TYPE AGV TRANSPORT SYSTEMS

Data entry	Value
Product interval T_I [s] (per 50 s)	200–500
AGV speed [m/s]	1
Number of AGVs	4
Experiment time [s]	28,000
Warm-up time [s]	2,000

VI. EXPERIMENTAL PROCEDURE OF SLAM OPERATIONS

A. Purpose of Experiment

In experiments using SLAM, it is important to estimate the self-position at a high level, which is closely related to the problem of interference between AGVs. The accuracy of the self-position estimations may depend on the environment and speed of the AGVs in which they are used. Therefore, this experiment investigates the accuracy of self-position estimation when the environment and speed at which the AGVs are used vary.

B. Experimental Device

In an experiment using SLAM, the Megarover Ver. 3.0, manufactured by the Viston Corporation, was used as the actual device. A photograph of the Megarover Ver. 3.0 and its plan view are presented in Figs. 8 and 9, respectively. A light detection and ranging (LiDAR) sensor manufactured by Shenzhen EAI Technology was attached to the front of the vehicle. A computer running Ubuntu 20.04 with a 4096-ppr resolution encoder and ROS Noetic was also installed. Subsequently, the mapping was performed.

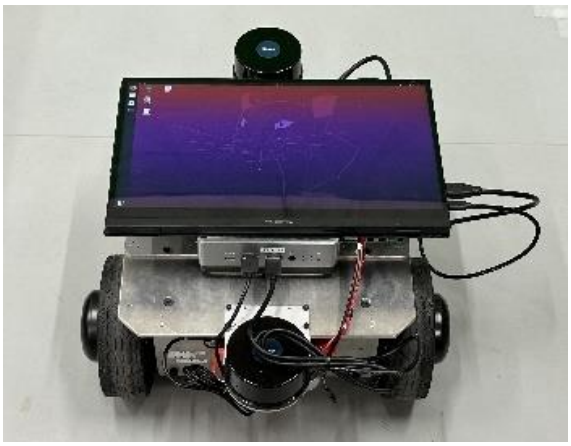

Fig. 8. Megarover ver. 3.0.

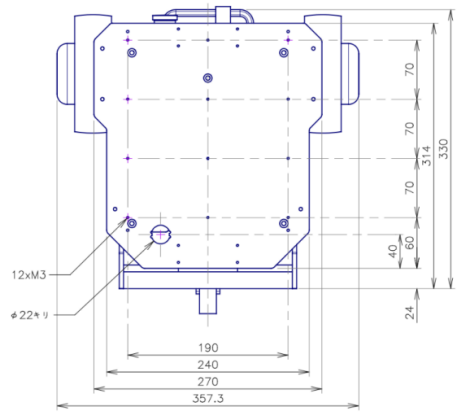

Fig. 9. The drawing of megarover ver. 3.0.

C. Flow Path Model Setup

Fig. 10(a) and (b) illustrate the flow path models used in the experiments. The course length was set to 3 m, and the course width was set to 2.0 m in accordance with Japanese occupational safety and health regulations. Two types of courses were used in the experiment because of the possible influence of walls and other features: (a) walls along both ends in the x-direction and (b) walls on all four sides.

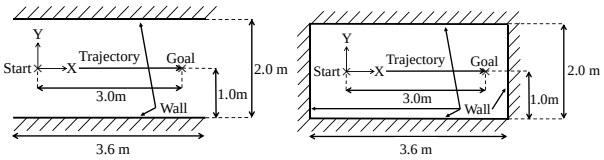

(a) Both sides of wall (b) Rectangles of wall

Fig. 10. Flow path model of SLAM.

D. Experimental Conditions

The experimental conditions are listed in Table V. Twist-type commands were sent as speed commands, and the AGV was operated at a trapezoidal speed of 3.0 m. The magnitude of acceleration and deceleration, a [m/s^2], of the trapezoidal velocity, was set to 0.20 m/s^2 to match the response performance of Megarover Ver. 3.0. Experiments were conducted by varying the velocity v [m/s] in 0.10 m/s increments from 0.10 m/s to 0.60 m/s when it became constant. First, each course was mapped using gmapping to obtain the coordinates for self-position estimation. Next, trapezoidal velocity commands were executed for each speed on (a) both sides of the wall and (b) rectangular courses, and the standard deviation of the self-position coordinates at each time was measured by moving straight ahead on a 3.0 m course. The standard deviation of the self-position-estimated coordinates represents the accuracy of the self-position estimation; the smaller the standard deviation, the higher the self-position estimation accuracy. Therefore, the standard deviation was used as the evaluation function, as expressed in Eq. (5).

$$S_x = \sqrt{\frac{\sum_{i=1}^{n} x_i^2 \Pi_i}{\sum_{i=1}^{n} \Pi_i} - \left(\frac{\sum_{i=1}^{n} \Pi_i x_i}{\sum_{i=1}^{n} \Pi_i}\right)^2} \quad (5)$$

In Eq. (5), n is the number of particles, x is the x-coordinate of each particle, and Π is the likelihood of each particle.

TABLE V. EXPERIMENTAL CONDITIONS OF SLAM EXPERIMENT

Data entry	Value	
Command speed v [m/s]	0.10–0.60 (per 0.10)	
Acceleration a [m/s^2]	0.20	
Trajectory	Straight path	
Wall	Both sides	Rectangle

VII. RESULTS AND DISCUSSION

A. Relation between Product Interval and Interference Time Rate

Fig. 11 illustrates the relationship between the product interval and the interference time rate for the normal control and each divided control. Comparing the normal and divided controls, the interference time rate was lower in the divided control group, particularly in two cases. The difference between normal control and taxi-type AGV control is that the normal control waits at the destination P/D after transport, whereas the taxi-type AGV control with clustering waits and operates while the AGV cruises. One disadvantage of normal controls is that a standby P/D cannot be selected after transport. By contrast, through clustering, taxi-type AGVs can use relatively distant P/Ds as standby P/Ds. Therefore, even if a P/D is selected as standby, the possibility of other AGVs using a nearby route is low, and interference is unlikely. In addition, when divided into two controls, no waiting operation is performed, and only the cruising operation is performed. Therefore, the interference time rate was considered very small and divided into two controls. Thus, taxi-type AGVs with clustering are considered excellent transport systems that can reduce interference more effectively than normal controls.

Fig. 11 demonstrates that in the case of a layout without a passing place, the larger the product interval, the larger the interference time rate. Fig. 11(c) and (d) illustrate that the interference time rate for the layout with the passing place is lower than that for the layout without the passing place, irrespective of the product interval. This suggests that the primary cause of interference is when the AGV is waiting at P/D, which is one of two cases: interference between AGVs passing through intersections and interference between AGVs waiting at P/Ds. This suggests that the primary cause of interference is the AGV waiting at the P/D. Suppose another AGV is already waiting at the P/D to which it is moving. In that case, it cannot move the goods to be conveyed, and the interference continues until the AGV already waiting starts moving according to the next command. Therefore, the interference time rate is considered larger when the product interval is large. Therefore, installing the passing location was effective, regardless of the product interval. The installation of the passing place was also found to have a significant effect on the interference time rate because the larger the product interval, the more the interference time rate was reduced by installing the passing place.

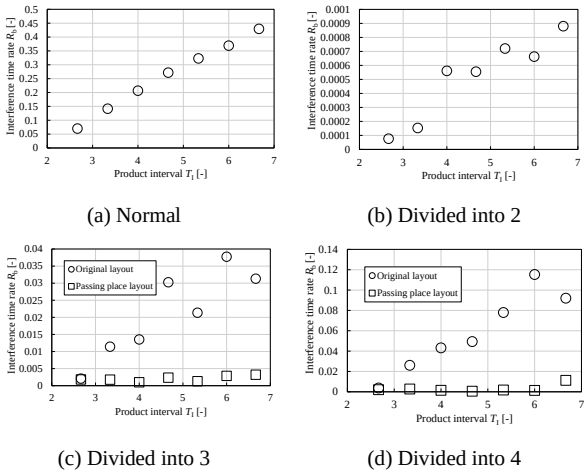

(a) Normal (b) Divided into 2

(c) Divided into 3 (d) Divided into 4

Fig. 11. Relationship between product interval and interference time rate R_b.

B. Relationship between Velocity, Feature Values, and Self-Location Estimation Accuracy

Fig. 12 illustrates the relationship between the velocity v [m/s] and standard deviation S_x [m] of the last transmitted self-position estimated coordinates for (a) both sides of the wall and (b) the rectangle. Because the initial value of the standard deviation is a process of sampling particles and converging to some extent as the AGV moves, the final standard deviation that was transmitted was used for evaluation. Fig. 12 presents that the overall standard deviation is smaller for rectangle (b) than for both sides (a). Thus, the final self-position estimation accuracy is higher for rectangle (b), and it is effective to place features such as walls to achieve higher accuracy in self-positioning. Fig. 12 also demonstrates that the standard deviation increases with increasing speed, particularly in the case of (a) both sides of the wall. This indicates that the higher the speed, the lower the self-position estimation accuracy. The low accuracy of the self-position estimation increases the likelihood of interference between AGVs. Therefore, depending on the environment in which AGVs are used, it is necessary to increase the accuracy of self-position estimation by placing objects with feature values, such as walls, when AGVs are used at higher traveling speeds. Fig. 12 also demonstrates that S_x was less than 0.16 m for all experimental conditions. In other words, the variation of the self-estimated position in the direction of travel is less than 0.16 m. Therefore, if the distance between AGVs can be maintained larger than this self-estimated position variation, interference between AGVs can be avoided.

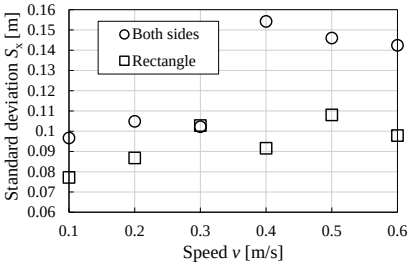

Fig. 12. Relationship between speed v and standard deviation S_x.

VIII. Conclusion

We proposed the installation of the passing place to avoid interference between AGVs during autonomous operations. We also used SLAM to investigate how the accuracy of the self-position estimation varied depending on the actual speed of the AGVs and the environment in which they were used. There was a positive correlation between the interval between the product interval and the interference time rate. The interference time rate was significantly reduced by installing a waiting area. Therefore, it was found that the main cause of interference was when the taxi-type AGV waited at the P/D, and installing the passing place was effective. In the SLAM experiment, speed and standard deviation were positively correlated. The standard deviation was smaller for the rectangle (b) than the wall (a) on both sides. Therefore, the possibility of interference between AGVs increases when the speed is high or when there are few features, such as walls, because the accuracy of self-position estimation decreases.

Conflict of Interest

The authors declare no conflict of interest.

Author Contributions

Tomoya Matsui and Yasuaki Omi conducted this research. Tomoya Matsui analyzed the data and wrote this paper. All authors had approved the final version.

Acknowledgment

The authors are grateful for the research environment at Doshisha University. We also grateful to the referees for useful comments.

References

[1] P. Valckenaersa and H. Van B, "Holonic manufacturing execution systems," *CIRP Ann. Manuf. Technol.*, vol. 54, pp. 427–432, 2005.
[2] K. Sugito, T. Inoue, M. Kamijima, S. Takeda, and T. Yokoi, "The protean production system as a method of improving production system responsiveness," in *Proc. Manufacturing Systems Division Conference*, 2004, vol. 70, no. 6, pp. 737–741. (in Japanese)
[3] R. Tujii, H. Yamamoto, and T. Yamada, "Production simulation of autonomous decentralized FMS including AGVs with different personalities of mind," in *Proc. ICAROB*, 2018, pp. 43–46.
[4] K. Uejo, H. Yamamoto, and T. Yamada, "Autonomous decentralized FMS that adopts priority order structure based on AGV's lie," in *Proc. ICAROB*, 2019, pp. 614–617.
[5] H. Yamamoto, "A'Vs' action decision by future foresee reasoning in decentralized autonomous FMS," *Transactions of the Japan Society of Mechanical Engineers. C*, vol. 65, no. 631, pp. 1281–1287, 1990 (in Japanese).
[6] T. Higashi, K. Sekiyama, and T. Fukuda, "An autonomous strategy formation in the AGV transport system," *Transactions of the Japan Society of Mechanical Engineers. C*, vol. 65, no. 629, pp. 185–191, 1999. (in Japanese)
[7] N. Murayama and S. Kawata, "A genetic algorithm approach to simultaneous scheduling of processing machines and multiple-load automated guided vehicles," *Transactions of the Japan Society of Mechanical Engineers. C*, vol. 71, no. 712, pp. 304–309, 2005. (in Japanese)
[8] N. Murakami and S. Kawata, "A genetic algorithm approach to simultaneous scheduling of processing machines and multiple-load automated guided vehicles," *Transactions of Japan Society of Mechanical Engineers, Series of C*, vol. 71, no. 712, pp. 304–309, 2005. (in Japanese)
[9] T. Oi, "Traffic flow model of cellular automation research," *Institute for mathematical Science* (2010), pp. 94–99 (in Japanese).
[10] K. Nishinari, "Cellular automaton models of traffic flow," *Bulletin of the Japan Society for Industrial and Applied Mathematics*, vol. 12, no. 2, pp. 26–37, 2002. (in Japanese)
[11] R. Murai, T. Sakai, H. Uematsu, H. Nakajima, H. Mitani, and T. Kitano, "Practical design and use of transfer system by autonomous mobile robot group," *The Robotics Society of Japan*, vol. 28, pp. 311–318, 2010. (in Japanese)
[12] T. Watanuki, T. Nakamura, and M. Kaneko, "Autonomous accompanying robot which adjusts the relative position with companion properly under dynamic environment," *The Institute of Image Information and Television Engineers*, vol. 40, no. 5, pp. 53–56, 2016. (in Japanese)
[13] R. Nakawatase, Y. Hakanishi, M. Touge, and A. Kubota, "Relationship between sliding material and lubricating liquid in biomimetic bearing," *Bioengineering Division Conference*, vol. 23, pp. 173–174, 2011. (in Japanese)
[14] A. Hirano, M. SuZuki, T. Tsuji, N. Takiguchi, and Ohtake, "Bio-mimetic control of mobile robots based on paramecium model," in *Proc. The JSME Bioengineering Conference and Seminar*, vol. 17, pp. 339–340, 2005. (in Japanese)
[15] Y. Dobrev, M. Vossiek, M. Christmann, I. Bilous, P. Gulden, "Wireless local positioning systems for tracking and autonomous navigation of transport vehicles and mobile robots," *IEEE Microwave Magazine*, vol. 18, no. 6, pp. 32–33, 2017.
[16] A. Mizoe, M. Furukawa, E. Miyawaki, M. Watanabe, I. Suzuki, and M. Yamamoto, "A study on order picking navigation in a large-scale logistic center," *Precision Engineering Journal*, vol. 75, no. 10, pp. 1260–1261, 2009. (in Japanese)
[17] D. F. Chen, Y. H. Hua, "Research on ROS -based AGV navigation system," *International Core Journal of Engineering*, vol. 3, no. 11, pp. 254–268, 2017.
[18] K. Kobayashi, T. Hirogaki, E. Aoyama, K. Ogawa, and T. Takahashi, "Route estimation by network voronoi diagram in taxi-type AGV control," in *Proc. International Symposium on Flexible Automation (ISFA)*, 2018, pp. 165–170.
[19] S. Kram, V. Lehtola, and G. Vosselman, "Strategies to integrate IMU and lidar SLAM for indoor mapping," *ISPRS*, vol. 1, pp. 223–230, 2020.
[20] D. Frank, F. Dieter, B. Wolfram, and T. Sebastian, "Monte Carlo localization for mobile robots," in *Proc. IEEE Int. Conf. on Robotics and Automation (ICRA)*, 1999, pp. 1322–1328.
[21] M. Tomonou, "Probabilistic self-location estimation and map construction for mobile robots," *Journal of the Robotics of Japan*, vol. 29, no. 5, pp. 423–426, 2011. (in Japanese)
[22] N. Harada, T. Nakatani, T. Hirogaki, and E. Aoyama, "Design of distributed route based on un-utility coefficient under an uncertain transportation condition at logistics center for autonomous AGVs," *Int. J. of Mechanical Engineering and Robotics Research*, vol. 12, no. 1, pp. 8–15, 2023.